

Outage and Capacity of Heterogeneous Cellular Networks with Intra-tier Dependence

Na Deng, Wuyang Zhou

Dept. of Electronic Engineering and Information Science
University of Science and Technology of China
Hefei, Anhui, 230026, China
Email:ndeng@mail.ustc.edu.cn, wyzhou@ustc.edu.cn

Martin Haenggi

Dept. of Electrical Engineering
University of Notre Dame
Notre Dame, IN, 46556, USA
Email:mhaenggi@nd.edu

Abstract—In this paper, we propose a two-tier heterogeneous cellular network (HCN) model with intra-tier dependence, where the macro base stations (MBSs) and the pico base stations (PBSs) follow a Poisson point process (PPP) and a Matern cluster process (MCP), respectively. Due to the high spatial fluctuations of the traffic demand, the users are modeled as a Cox process. Conditioning on a fixed distance between a user equipment (UE) and its nearest serving BS, exact calculations of the interference and the outage probability are derived. The per-user capacity and the area spectral efficiency are also analyzed. The results show that the model with intra-tier dependence appears closer to the real deployment than the extreme with the complete randomness (the PPP). An important conclusion is that both the per-user capacity and the area spectral efficiency improve with smaller cells, but outage does not.

I. INTRODUCTION

With the rapid increase of mobile subscribers as well as the traffic demand, the thoroughly planned architecture comprised of macrocells designed to cater to large coverage regions is evolving towards a much more heterogeneous architecture where the macrocell network is overlaid by diverse kinds of small cells deployed in an irregular and unplanned fashion using universal frequency reuse [1]. This increasing heterogeneity and density in cellular networks renders the traditional hexagonal and regular deployment models of limited utility but, in turn, motivates recent studies, tools and results inspired by stochastic geometry [2–4].

By far the most common assumption used in analytical calculations for heterogeneous cellular networks (HCNs) is that base stations (BSs) in different tiers follow mutually independent homogeneous Poisson point processes (PPPs) [5–7]. This means that the BSs are located independently of each other and their spatial correlation is ignored. Although the assumption of Poisson processes makes the analysis tractable, it does not seem realistic because of the uneven population distributions and the practical BSs deployment with an objective (say, coverage-centric or capacity-centric) being strongly associated with human activities, which leads to dependence among the BSs including inter-tier dependence (i.e., the BSs belonging to different tiers exhibit repulsion) and intra-tier dependence (i.e., the BSs within a tier are not totally independent but planned deployments with a degree of randomness due to irregular terrains and hotspots).

This motivates the approach of devising and analyzing HCN models accounting for the spatial dependence. To our best knowledge, very few articles have proposed a stochastic geometry-based model considering inter-tier or intra-tier dependence for HCNs: [8] proposes two spatial models of HCNs according to the Ginibre point process (GPP) [9] whose points exhibit repulsion and accounts for the repulsion among the BSs in different tiers and that in the same tier, respectively. Our previous work [10] proposes a two-tier HCN model with inter-tier dependence, where the MBSs and the PBSs follow a PPP and a Poisson hole process, respectively. Both [8] and [10] focus on the repulsion among the BSs but, in fact, due to the human activities and high spatial fluctuations in traffic demand, the actual BSs in cellular networks are deployed densely in some places, exhibiting clustering behavior, and sparsely in other places. Therefore, for HCNs, where small cells are primarily added to increase capacity in hotspots with high user demand, it is unnecessary to add small cells to every macrocell but to place them in regions where an MBS cannot offer enough capacity. This is the motivation of our work.

In this paper, we consider a more practical HCN and focus on the intra-tier dependence, where the traffic load can have significant spatial fluctuations and clusters of PBSs are placed in hotspot regions. Under this scenario, we propose a two-tier HCN model with two types of BSs, i.e., MBSs and PBSs, following a PPP and an independent Matern cluster process (MCP) [2], respectively. Thereby, the intra-tier dependence is reflected by the MCP whose points exhibit clustering behavior. For the user distribution, the user density in hotspot regions is higher than in the rest of the network, and thus the users in the whole network form a Cox process [2]. Conditioning on a fixed distance between a user equipment (UE) and its nearest serving BS, exact expressions of the interference and the outage probability are derived. The per-user capacity and the area spectral efficiency are also analyzed. We then compare the proposed model with the two-tier independent PPPs model through numerical experiments to show the effect of the intra-tier dependence on different performance metrics.

From a broader perspective, the contribution of the paper lies in the investigation of a novel model with intra-tier dependence for HCNs, which is applicable to actual network deployments, especially for those having hotspots with high

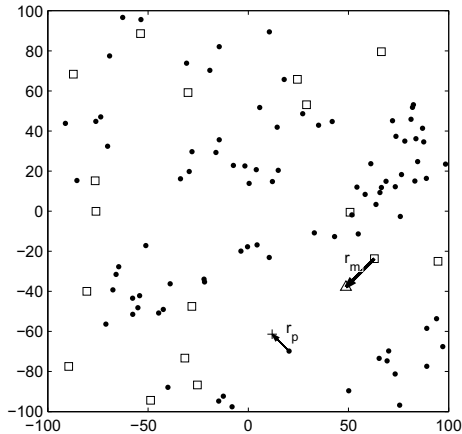


Fig. 1. The two-tier HCN model with intra-tier dependence. The squares are the MBSs and the triangle is the typical MU at a distance r_m from its serving MBS in a random direction. The dots are the PBSs and the '+' is the typical PU at a distance r_p from its serving PBS in a random direction.

user density.

II. NETWORK MODEL

Consider a two-tier HCN with two types of BSs: MBSs and PBSs, shown in Figure 1. The locations of the active MBSs follow a homogeneous PPP $\Phi_m = \{x_1, x_2, \dots\} \subset \mathbb{R}^2$ of density λ_m , and the locations of the PBSs follow an independent MCP $\Phi_p = \{y_1, y_2, \dots\} \subset \mathbb{R}^2$ with the parent point process Φ_l with density λ_l . Denoting the average number of points per cluster as \bar{c} , the density of the PBSs can be expressed as $\lambda_p = \lambda_l \bar{c}$. Points in each cluster are uniformly distributed in the circle of radius R centered at its parent point. For the user distribution, it is assumed that the user density in those regions (i.e., the hotspots) covered by PBSs is higher than in the rest of the network. Specifically, the population centers of radius R are assumed to be Poisson distributed and the active user, i.e., the pico user (PU), density in these centers is $\bar{c}/(\pi R^2)$. These population centers are covered using PBSs forming a MCP such that (on average) each PU can be served by its own PBS. The macro users (MUs) distributed in the rest of the network are served by their own MBSs. To facilitate the calculation, we assume that each PBS serves one PU and each MBS serves one MU in one resource block at a time, thus the densities of MUs and PUs are equal to that of MBSs and PBSs, respectively. Under this setup, the total UEs in the network form a Cox process with density $\lambda_m + \lambda_p$, which are clustered in hotspots and uniformly distributed in the rest.

The transmit power is μ_m for each MBS and μ_p for each PBS. The power received by a receiver located at z due to a transmitter at x is modeled as $h_x \ell(x - z)$, where h_x is the power fading coefficient (square of the amplitude fading coefficient) associated with the channel between x and z . We assume that the fading coefficients are i.i.d. exponential

(Rayleigh fading) with $\mathbb{E}[h] = 1$. $\ell(x) = \|x\|^{-\alpha}$ is the large-scale path loss model with $\alpha > 2$. We focus on an MU at a distance r_m from the serving MBS in a random direction and a PU at a distance r_p from the serving PBS in a random direction. The signal-to-interference ratio (SIR) threshold is denoted as θ_m for MUs and θ_p for PUs.

III. ANALYSIS OF THE TWO-TIER HCN MODEL WITH INTRA-TIER DEPENDENCE

In this section, we first analyze the aggregate interference to both MUs and PUs, including the intra-tier interference and the inter-tier interference, and then give the outage probability, the per-user capacity and the area spectral efficiency, respectively.

There are four types of interference: the interference from the MBSs to the MUs I_{mm} , the interference from the MBSs to the PUs I_{mp} , the interference from the PBSs to the MUs I_{pm} , and the interference from the PBSs to the PUs I_{pp} . Each of them can be defined as $I(z) = \sum_{x \in \Phi \setminus \{x_0\}} \mu h_x \ell(z - x)$ to represent the interference at z resulting from the interferers positioned at the points of the process Φ (i.e., either Φ_m or Φ_p), where x_0 is the serving BS, and μ is either μ_m or μ_p , depending on which type of interference is considered. To calculate the interference to the MUs, we condition on having a MU at the origin, the *typical user*, i.e., there is an extra MBS, namely, the serving MBS, on the circle of radius r_m centered at o , which yields the Palm distribution for the MBSs. By Slivnyak's theorem [2], this conditional distribution is the same as the original one for the macro-tier in the region $\mathbb{R}^2 \setminus b(o, r_m)$. For the pico-tier, we also condition on having a typical PU at the origin, which is the same as the macro-tier.

A. Interference and Outage Analysis of MUs

The MUs suffer from two types of interference: I_{mm} and I_{pm} . The typical MU is assumed to access the nearest MBS x_0 at distance r_m . Since the fading is Rayleigh and the MBSs are distributed as a PPP, the Laplace transform of I_{mm} is

$$\begin{aligned} \mathcal{L}_{I_{mm}}(s) &= \mathbb{E}_{\Phi_m, h_x}^{!x_0} \left(\exp \left(-s \sum_{x \in \Phi_m} \mu_m h_x \ell(x) \right) \right) \\ &= \mathbb{E}_{\Phi_m}^{!x_0} \left(\prod_{x \in \Phi_m} \frac{1}{1 + s \mu_m \ell(x)} \right) \\ &\stackrel{(a)}{=} \exp \left(-\lambda_m \int_{\mathbb{R}^2 \setminus b(o, r_m)} 1 - \frac{1}{1 + s \mu_m \ell(x)} dx \right) \\ &\stackrel{(b)}{=} \exp \left\{ -\pi \lambda_m \frac{\mu_m s \delta}{1 - \delta} r_m^{2-\alpha} F(1, 1 - \delta; 2 - \delta; -\mu_m s r_m^{-\alpha}) \right\}, \end{aligned} \quad (1)$$

where $\delta = 2/\alpha$, (a) follows from the probability generating functional (PGFL) of the PPP, and the integration regions is $\mathbb{R}^2 \setminus b(o, r_m)$ since the closest interferer is at least at a distance r_m . $F(x, y; z; w)$ is the hypergeometric function [11] and (b) can be obtained with the help of equation (3.194.5) in [11] and polar coordinates.

Let $\mathcal{L}_{I_{\text{pm}}}(s)$ be the Laplace transform of the interference from a MCP at the typical MU located at the origin. According to [2, Cor. 4.13], we have

$$\mathcal{L}_{I_{\text{pm}}}(s) = \exp \left\{ -\lambda_l \int_{\mathbb{R}^2} [1 - \exp(-\bar{c}\nu(s, y))] dy \right\}, \quad (2)$$

where $\nu(s, y) = \int_{\mathbb{R}^2} \frac{f(x)}{1 + (s\mu_p \ell(x-y))^{-1}} dx$, and $f(x)$ is the PDF of the node distribution around the parent point. For the MCP,

$$f(x) = \begin{cases} \frac{1}{\pi R^2}, & \|x\| < R \\ 0, & \text{otherwise.} \end{cases} \quad (3)$$

With Rayleigh fading, the transmission success probability of the MU is the Laplace transform evaluated at $s = \theta_m \mu_m^{-1} r_m^\alpha$. Since Φ_m and Φ_p are independent, I_{mm} and I_{pm} are independent. Therefore, the outage probability of the MU is

$$\epsilon_m = 1 - \mathcal{L}_{I_{\text{mm}}}(\theta_m \mu_m^{-1} r_m^\alpha) \mathcal{L}_{I_{\text{pm}}}(\theta_m \mu_m^{-1} r_m^\alpha). \quad (4)$$

B. Interference and Outage Analysis of PUs

Similar to the case of estimating the interference to the MUs, the PU also experiences two types of interference: I_{mp} and I_{pp} . First, we consider the interference from other PBSs I_{pp} . Let $\mathcal{L}_{I_{\text{pp}}}(s)$ be the Laplace transform of the interference from a MCP at the typical PU located at the origin. Since the typical PU is served by the nearest PBS located at $(r_p, 0)$, there is no PBS in the disk region centered at the origin with radius r_p . Thus, using the modified path loss law $\ell(x) = \ell(x) \mathbf{1}_{\|x\| > r_p}$ and according to Eq. (34) in [12], we have

$$\mathcal{L}_{I_{\text{pp}}}(s) = \exp \left\{ -\lambda_l \int_{\mathbb{R}^2} [1 - \exp(-\bar{c}\nu(s, y))] dy \right\} \times \int_{\mathbb{R}^2} \exp(-\bar{c}\nu(s, y)) f(y) dy, \quad (5)$$

where $\nu(s, y) = \int_{\mathbb{R}^2} \frac{f(x)}{1 + (\bar{c}\ell(x-y)s\mu_p)^{-1}} dx$.

Now let us consider the interference from the MBSs I_{mp} . Let $\mathcal{L}_{I_{\text{mp}}}(s)$ be the Laplace transform of the interference from a PPP at the typical PU located at the origin and we have $\mathcal{L}_{I_{\text{mp}}}(s) = \exp\left(-\lambda_m \frac{\pi^2 \delta}{\sin(\pi \delta)} \mu_m^\delta s^\delta\right)$. The success probability of PUs is the Laplace transform evaluated at $s = \theta_p \mu_p^{-1} r_p^\alpha$. Since I_{mp} and I_{pp} are independent, the outage probability of the PU is

$$\epsilon_p = 1 - \mathcal{L}_{I_{\text{mp}}}(\theta_p \mu_p^{-1} r_p^\alpha) \mathcal{L}_{I_{\text{pp}}}(\theta_p \mu_p^{-1} r_p^\alpha). \quad (6)$$

C. Per-user Capacity and Area Spectral Efficiency

According to our network model, since the densities of MUs and PUs are equal to that of MBSs and PBSs, respectively, and the PUs are concentrated in the densely populated regions, the MUs take the proportion $\kappa_m = \frac{\lambda_m}{\lambda_m + \lambda_p}$ of the total UEs and the proportion of PUs is $\kappa_p = 1 - \kappa_m$. Then, we obtain the per-user capacity of the MU and PU for a fixed-rate transmission based on the SIR threshold, respectively, as follows,

$$c_m = (1 - \epsilon_m) \log_2(1 + \theta_m) \quad (7)$$

$$c_p = (1 - \epsilon_p) \log_2(1 + \theta_p) \quad (8)$$

Thus, the per-user capacity c_u can be derived as

$$c_u = \kappa_m c_m + \kappa_p c_p = \frac{\lambda_m(1 - \epsilon_m) \log_2(1 + \theta_m) + \lambda_p(1 - \epsilon_p) \log_2(1 + \theta_p)}{\lambda_m + \lambda_p}. \quad (9)$$

Finally, the area spectral efficiency (ASE) of the proposed model with intra-dependence can be defined as [13]

$$\text{ASE} = \lambda_m(1 - \epsilon_m) \log_2(1 + \theta_m) + \lambda_p(1 - \epsilon_p) \log_2(1 + \theta_p). \quad (10)$$

D. Comparison with the Two-tier Independent PPP Model

Compared with the two-tier independent PPP model, i.e., the MBSs and PBSs follow two mutually independent homogeneous PPPs with the same densities λ_m and λ_p , respectively, the only difference from our proposed model is that the PBSs are distributed as a homogeneous PPP. Under the same user distribution, in order to make this comparison relatively fair, we assume that at least one PBS is located in each hotspot region and hence model the PBSs in the two-tier independent PPP model as the superposition of Φ_l and another independent homogeneous PPP Φ'_p with density $\lambda_l(\bar{c} - 1)$.

First, the outage probability of the MU can be easily obtained as

$$\epsilon_m = 1 - \exp \left\{ -\pi \lambda_m \frac{\theta_m \delta}{1 - \delta} r_m^2 F(1, 1 - \delta; 2 - \delta; -\theta_m) - \frac{\pi^2 \delta \theta_m^\delta}{\sin(\pi \delta)} r_m^2 \lambda_p \left(\frac{\mu_p}{\mu_m} \right)^\delta \right\}. \quad (11)$$

Then, for those PUs that actually have a serving PBS, the outage probability is

$$\epsilon_p^s = 1 - \exp \left\{ -\frac{\pi^2 \delta \theta_p^\delta}{\sin(\pi \delta)} r_p^2 \lambda_m \left(\frac{\mu_m}{\mu_p} \right)^\delta - \pi \lambda_p \frac{\theta_p \delta}{1 - \delta} r_p^2 F(1, 1 - \delta; 2 - \delta; -\theta_p) \right\}, \quad (12)$$

and the outage probability of the PU not served (i.e. blocked) is $\epsilon_p^b = 1$. Since $\Phi_p = \Phi_l + \Phi'_p$, there are $N_p = \frac{\lambda_l(\bar{c}-1)}{\lambda_l + \lambda_m} + 1$ PBSs on average in each hotspot region to serve the \bar{c} PUs. Thus, the outage probability of an arbitrary PU can be derived as

$$\epsilon_p = \frac{N_p}{\bar{c}} \epsilon_p^s + 1 - \frac{N_p}{\bar{c}} \quad (13)$$

Note that when $\bar{c} = 1$, our proposed model and the two-tier independent PPP model are the same. And for the latter, as \bar{c} increases, the number of PUs that are actually served will decrease until when $\bar{c} \rightarrow \infty$, the proportion of the served PUs reaches the minimum of $\frac{\lambda_l}{\lambda_m + \lambda_l}$.

For the per-user capacity, we have $c_m = (1 - \epsilon_m) \log_2(1 + \theta_m)$ for the MU and $c_p = (1 - \epsilon_p) \log_2(1 + \theta_p)$ for the PU, respectively. Thus, the per-user capacity for the two-tier independent PPP model is

$$c_u = \frac{\lambda_m(1 - \epsilon_m) \log_2(1 + \theta_m) + \lambda_p(1 - \epsilon_p) \log_2(1 + \theta_p)}{\lambda_m + \lambda_p}. \quad (14)$$

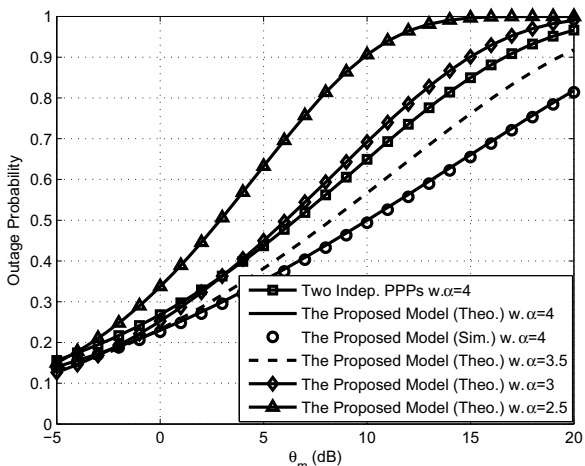


Fig. 2. The outage probability of MUs.

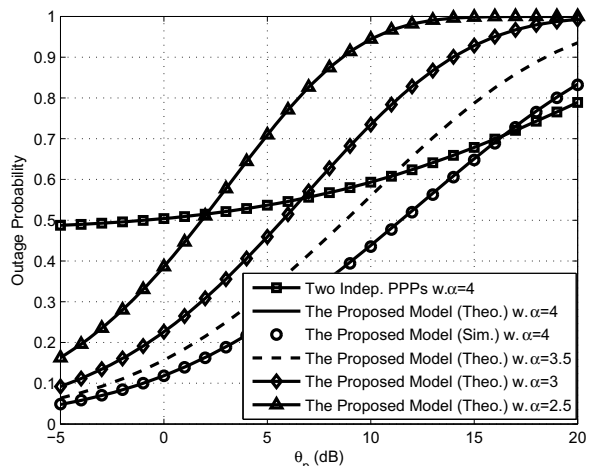


Fig. 3. The outage probability of PUs.

Finally, the ASE for the two-tier independent PPP model is defined as

$$\text{ASE} = \lambda_m(1-\epsilon_m) \log_2(1+\theta_m) + \lambda_p \frac{N_p}{\bar{c}} (1-\epsilon_p^s) \log_2(1+\theta_p). \quad (15)$$

IV. NUMERICAL RESULTS

In this section, we give some numerical results of the outage probability for MU and PU, the per-user capacity, and the area spectral efficiency, respectively, where $\lambda_m = \lambda_l = 8 \times 10^{-6}$, $\mu_m = 1$, $\mu_p = 0.05$, $r_m = 40$, $r_p = 10$, $\alpha = 4$, $\bar{c} = 20$, $R = (\pi(\lambda_m + \lambda_l))^{-1/2}$. As a baseline, we also provide the performance of the two-tier independent PPP model with the same densities of the MBSs and the PBSs, and the same user distribution to show the effect of the intra-tier dependence on different performance metrics.

Figure 2 and 3 illustrate the outage probabilities of MUs and PUs, respectively, for different path-loss exponents α , where the simulation result matches the analytical result well, thus corroborating the accuracy of our theoretical analysis. We can observe that for both MUs and PUs, the model with larger α has better outage performance due to the fast attenuations of the interference signals. For the MU, the outage performance of the proposed model with intra-tier dependence is superior than that of the two-tier independent PPP model; while for the PU, significant gains are obtained by the proposed model when θ_p is small and the outage probability of the two-tier independent PPP model starts from 0.5, which is consistent with the theoretical analysis in Section III-D due to the parameter settings in the simulations¹. When θ_p increases larger enough, say $\theta_p > 15\text{dB}$, the outage performance of the proposed model suffers much more serious deterioration than that of the independent model due to the greater interference caused by the clustering behavior among the PBSs even though the proposed model can serve more users (but, actually, most

of them suffer the outage), leading to the inferior outage performance than the independent model.

Figure 4 shows the relationship between the per-user capacity and the user threshold ($\theta_m = \theta_p = \theta$) for different average numbers of PBSs per cluster \bar{c} . We can observe that for both models, i.e., the proposed model and the two-tier independent PPP model, the model with smaller \bar{c} has higher per-user capacity. For the former, smaller \bar{c} means smaller number of PBSs per cluster, causing less interference from the PBSs, thus both the MU and PU have smaller outage probability and further increase the per-user capacity; while for the latter, since there are not enough PBSs for the many users in hotspot regions, the smaller the number of the PUs is, the higher per-user capacity can be obtained. Furthermore, for each case of \bar{c} , the proposed model has higher per-user capacity than the two-tier independent PPP model which indicates that the model with intra-tier dependence is a more appropriate model than the two-tier independent PPP model for the HCNs where the traffic demand exhibits high spatial fluctuations.

Figure 5 depicts how the ASE changes with the hotspot area fraction for different thresholds of both MUs and PUs. We set $\lambda_m + \lambda_l = 1.6 \times 10^{-5}$, then changing λ_l can be viewed as changing the ratio of the hotspot area to the whole network, i.e., the hotspot area fraction. It is seen that the ASE increases with λ_l . This is because, as λ_l increases, the hotspot area take more proportion in the network and the capacity provided by the PBSs increases, leading to the rise of the ASE. When $\lambda_l = 1.6 \times 10^{-5}$, i.e., the HCN degrades into a single-tier network only with the PBSs deployed, all curves reach the peak, which indicates that putting a cluster of small cells at some location in the network may indeed deteriorate the outage by the greater interference, but it will increase the ASE (which is related to the per-user capacity). Besides, the effect of the PU threshold θ_p on the ASE becomes more noticeable as λ_l increases while the MU threshold θ_m is not, because the increase of λ_l leads to more PBSs and less MBSs deployed, hence leading the PBSs to be the main provider of the network capacity. For

¹From (13), the proportion of the PUs that are actually served is $\frac{N_p}{\bar{c}} = \frac{\lambda_l}{\lambda_m + \lambda_l} + \frac{\lambda_m}{\lambda_m + \lambda_l} \frac{1}{\bar{c}}$. Since $\bar{c} = 20$ and $\lambda_l = \lambda_m$, the second term can be ignored. Thus, $\epsilon_p = 0.5\epsilon_p^s + 0.5$.

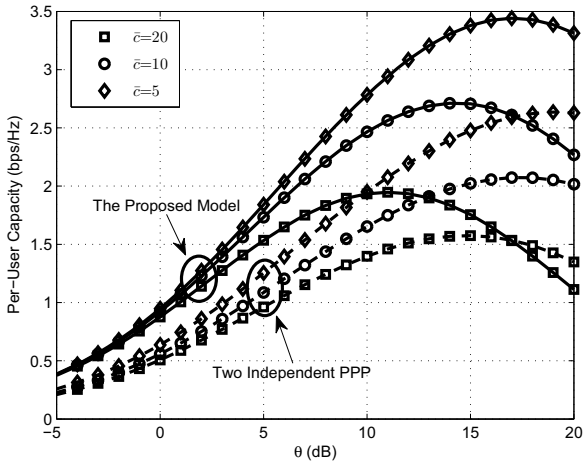


Fig. 4. Per-user capacity versus user threshold, where $\theta_m = \theta_p = \theta$.

the comparison between the proposed model and the two-tier independent PPP model, the result is similar to that of the per-user capacity.

V. CONCLUSION

In this paper, we proposed a two-tier HCN model accounting for intra-tier dependence, where traffic demand exhibits high spatial fluctuations and clusters of PBSs are placed in hotspot regions. By modeling the MBSs, the PBSs, and the users as a PPP, an independent MCP and a Cox process, respectively, and conditioning on a fixed distance between a UE and its nearest serving BS, exact calculations of the interference, the outage probability, the per-user capacity and the ASE were derived. The results indicate that the theoretical curves match the simulation results extremely well, thus corroborating the accuracy of the theoretical analysis. Besides, since for both outage and capacity, the proposed model is superior than the two-tier independent PPP model, we can conclude that the model with intra-tier dependence is a more promising and practical HCN model than the complete and independent randomness for actual network deployments with hotspots. Overall, both the per-user capacity and the ASE improve with smaller cells, but outage does not.

ACKNOWLEDGMENT

The work of N. Deng and W. Zhou has been supported by National programs for High Technology Research and Development (2012AA011402), National Natural Science Foundation of China (61172088), and the work of M. Haenggi has been supported by the U.S. NSF (grants CNS 1016742 and CCF 1216407).

REFERENCES

- [1] A. Ghosh *et al.*, "Heterogeneous cellular networks: From theory to practice," *Communications Magazine, IEEE*, vol. 50, no. 6, pp. 54–64, 2012.
- [2] M. Haenggi, *Stochastic geometry for wireless networks*. Cambridge University Press, 2012.

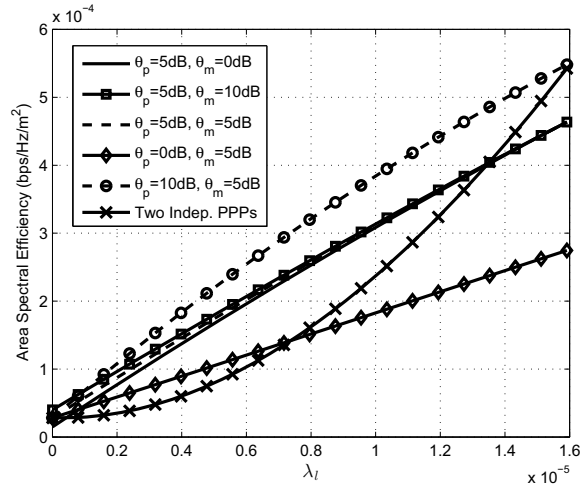


Fig. 5. Area spectral efficiency versus hotspot area fraction. For the two-tier independent PPP model, $\theta_m = \theta_p = 5\text{dB}$.

- [3] H. ElSawy, E. Hossain, and M. Haenggi, "Stochastic geometry for modeling, analysis, and design of multi-tier and cognitive cellular wireless networks: A survey," *Communications Surveys & Tutorials, IEEE*, vol. 15, no. 3, pp. 996–1019, 2013.
- [4] J. G. Andrews, R. K. Ganti, M. Haenggi, N. Jindal, and S. Weber, "A primer on spatial modeling and analysis in wireless networks," *Communications Magazine, IEEE*, vol. 48, no. 11, pp. 156–163, 2010.
- [5] H. S. Dhillon, R. K. Ganti, F. Baccelli, and J. G. Andrews, "Modeling and analysis of k-tier downlink heterogeneous cellular networks," *Selected Areas in Communications, IEEE Journal on*, vol. 30, no. 3, pp. 550–560, 2012.
- [6] S. Mukherjee, "Distribution of downlink SINR in heterogeneous cellular networks," *Selected Areas in Communications, IEEE Journal on*, vol. 30, no. 3, pp. 575–585, 2012.
- [7] G. Nigam, P. Minero, and M. Haenggi, "Coordinated Multipoint Joint Transmission in Heterogeneous Networks," *IEEE Transactions on Communications*, 2014, submitted. Available at <http://www.nd.edu/~mhaenggi/pubs/tcom14.pdf>.
- [8] I. Nakata and N. Miyoshi, "Spatial stochastic models for analysis of heterogeneous cellular networks with repulsively deployed base stations," *Performance Evaluation*, 2014.
- [9] N. Deng, W. Zhou, and M. Haenggi, "The Ginibre point process as a model for wireless networks with repulsion," *IEEE Transactions on Wireless Communications*, 2014, submitted. Available at <http://www.nd.edu/~mhaenggi/pubs/twc14c.pdf>.
- [10] —, "A heterogeneous cellular network model with inter-tier dependence," in *IEEE Global Communications Conference (GLOBECOM'14)*, Texas, USA, Dec. 2014, submitted. Available at <http://www.nd.edu/~mhaenggi/pubs/globecom14a.pdf>.
- [11] A. Jeffrey and D. Zwillinger, *Table of integrals, series, and products*. Academic Press, 2007.
- [12] R. Ganti and M. Haenggi, "Interference and outage in clustered wireless ad hoc networks," *Information Theory, IEEE Transactions on*, vol. 55, no. 9, pp. 4067–4086, 2009.
- [13] M. Haenggi, J. G. Andrews, F. Baccelli, O. Dousse, and M. Franceschetti, "Stochastic Geometry and Random Graphs for the Analysis and Design of Wireless Networks," *IEEE Journal on Selected Areas in Communications*, vol. 27, no. 7, pp. 1029–1046, Sep. 2009.